



Using yeast to sustainably remediate and extract heavy metals from waste waters

George L. Sun^{1,2}, Erin E. Reynolds³ and Angela M. Belcher^{1,2,4}

Our demand for electronic goods and fossil fuels has challenged our ecosystem with contaminating amounts of heavy metals, causing numerous water sources to become polluted. To counter heavy-metal waste, industry has relied on a family of physicochemical processes, with chemical precipitation being one of the most commonly used. However, the disadvantages of chemical precipitation are vast, including the generation of secondary waste, technical handling of chemicals and need for complex infrastructures. To circumvent these limitations, biological processes to naturally manage waste have been sought. Here, we show that yeast can act as a biological alternative to traditional chemical precipitation by controlling naturally occurring production of hydrogen sulfide (H_2S). Sulfide production was harnessed by controlling the sulfate assimilation pathway, where strategic knockouts and culture conditions generated H_2S from 0 to over 1,000 ppm (~30 mM). These sulfide-producing yeasts were able to remove mercury, lead and copper from real-world samples taken from the Athabasca oil sands. More so, yeast surface display of biomimetic peptides helped control for size distribution and crystallinity of precipitated metal sulfide nanoparticles. Altogether, this yeast-based platform not only removes heavy metals but also offers a platform for metal re-extraction through precipitation of metal sulfide nanoparticles.

Growing consumption of electronic goods and raw materials has pushed mining and manufacturing practices to such unprecedented levels that the United Nations Environment Programme declared a global waste challenge in 2015 to monitor waste risk and waste crimes¹. Because of the demand for metals, there was a cumulative 41.8 million metric tonnes (46.1 million tons) of electronic waste (e-waste) globally in 2014, which grew an additional 20–25% in 2018^{2,3}. In addition, the United States has more than 13,000 reported active mining sites with an additional 500,000 that are abandoned yet still polluting 16,000 miles of streams^{3,4}. Metal contaminants are typically copper, lead, cadmium, mercury and zinc⁵. Despite these obvious waste sources, industry still continues to unsustainably mine for raw materials, especially given the growing demand and consumption of batteries and electric vehicles⁶. China alone produces and consumes one of the largest quantities of batteries in the world, and in 2013 generated 570 kilotons of battery waste, with less than 2% being collected and recycled⁷. The main consequence of battery waste, especially from lithium-ion batteries, is the release of toxic amounts of copper and lead, with other metals such as cobalt, nickel and chromium leaching into neighbouring soils and streams⁶.

The advancement of remediation technologies, in particular heavy metal removal, is slow in comparison to the rise of e-waste and the pace of mining¹. So far, practical implementation of heavy metal remediation has relied on physicochemical treatments, the most ubiquitous method being chemical precipitation via lime, hydroxides (for example NaOH) or sulfides (for example FeS or H_2S)⁵. Sulfides have been the more desirable reagent for precipitation as they are more reactive and have a lower rate of leaching than hydroxide precipitates, but the counter is that sulfide gas storage and handling is dangerous and costly, making lime and hydroxides the preferred choice despite being less effective⁵. Overall, chemical precipitation is costly, requires dedicated infrastructure, involves

handling dangerous compounds and reactive gases, and generates secondary waste in the form of sludge^{5,8,9}. Furthermore, sludge is ineffectively eliminated through pyrolysis or physical transport to landfills for burial^{8,10}. Because of this, much of the precipitated waste leaches back into nearby water sources thereby perpetuating this cycle of inefficient cleaning. Thus, physicochemical treatment via chemical precipitation is not an amenable option for developing countries, which typically face the biggest challenge for heavy-metal removal¹⁰. Therefore, there is an urgent need to replace chemical precipitation with an alternative and more sustainable technology.

In contrast to physicochemical processes, scientists have discovered the benefits of using biological systems to remediate waste as a natural alternative. Bioremediation has gained traction for waste-water treatment due to its natural means to process waste in addition to its autonomous growth and environmentally friendly reactions^{11,12}. In addition, there is hope that with the growing tool kit of molecular biology and bioengineering technologies, scientists could further augment biology's capability to manipulate and convert waste. Already, scientists have discovered naturally occurring microorganisms that have been observed to tolerate and accumulate toxic metals, for example, metal-reducing microorganisms, particularly bacteria^{13–17}. One family of interest is sulfate-reducing microorganisms (SRMs), which use sulfate as their terminal electron acceptor to generate H_2S as a by-product, leading to precipitation of nearby metals. Connecting the dots, it is easy to see that biology has already developed a mechanism for biotic chemical precipitation using H_2S -producing SRMs. An interesting use of these organisms has been the design of anaerobic beds or stirred tank reactors for precipitation of metal-contaminated effluent^{18,19}. However, the limiting piece to this technology is the biology itself. SRMs are obligate anaerobes, require precise handling of culture conditions and grow slowly. In addition, many SRMs are unable to process complex carbon sources and require additional anaerobic microflora to persist²⁰,

¹Department of Biological Engineering, Massachusetts Institute of Technology, Cambridge, MA, USA. ²Koch Institute of Integrative Cancer Research, Massachusetts Institute of Technology, Cambridge, MA, USA. ³Department of Civil and Environmental Engineering, Massachusetts Institute of Technology, Cambridge, MA, USA. ⁴Department of Material Science, Massachusetts Institute of Technology, Cambridge, MA, USA. e-mail: belcher@mit.edu

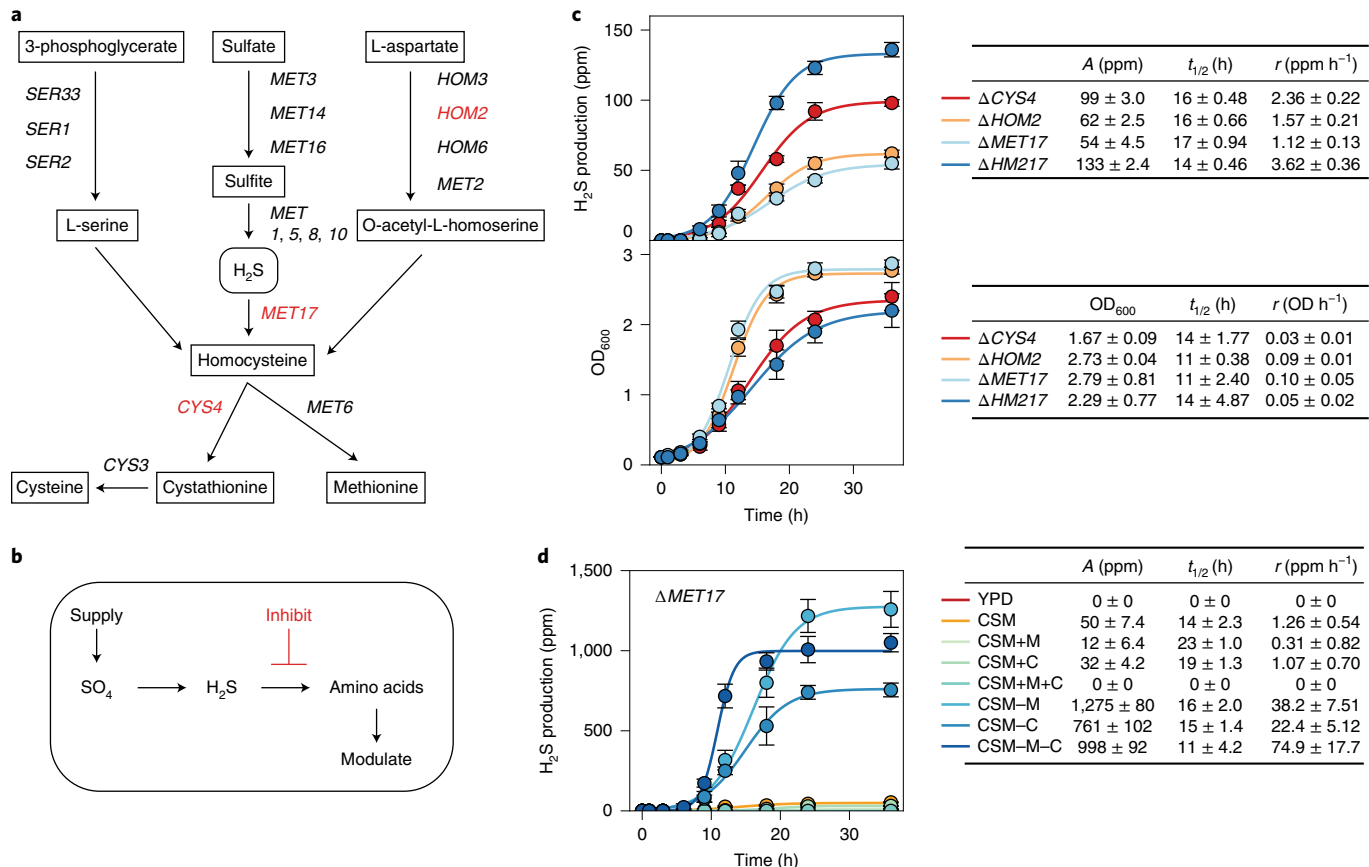


Fig. 1 | Engineering the yeast sulfate assimilation pathway to generate H₂S. **a**, Genes involved in the conversion of H₂S to amino acids were knocked out. Italicized knockouts were screened for H₂S production, while red knockouts gave noticeable production of H₂S. **b**, Deletant ΔCYS4, ΔHOM2, ΔMET17 and ΔHM217 produced sulfide, which followed Le Chatelier's principle as supplying sulfate (reactants), while limiting nutrients such as cysteine and methionine (products) motivated the production of sulfide. **c**, H₂S production (top curves) in relation to growth curves (bottom curves) in 50 ml CSM cultures. Fitted parameter A represents the steady-state production of H₂S, $t_{1/2}$ represents the time at which sulfide production reached half-max and r represents the maximum rate of H₂S production. **d**, H₂S production as a function of media composition for ΔMET17 with fitted parameters A, $t_{1/2}$ and r. For all data, the mean \pm s.d. of three replicates from different days are shown. Curves were fitted and parametrized against the sigmoid function $\frac{A}{1+e^{-k(t-t_0)}}$. Schematic in panel **a** adapted with permission from ref.³⁰, American Society of Microbiology.

creating an additional layer of complexity when managing reactors. To circumvent these stringent culture conditions, scientists have begun to extract and transfer SRMs' unique behaviour into more tractable organisms, such as *Escherichia coli*, by heterologously expressing enzymes and non-native metal-reducing pathways—a growing field of technology that uses genetically modified organisms (GMOs) for bioremediation applications²¹. Examples include the expression of the mercuric reductase genes from *Thiobacillus ferrooxidans* into *E. coli*²² or using combinations of protein and metabolic engineering to endow *E. coli* with sulfide-generating capabilities much like SRMs²³. Similar concepts have been developed in plants, such as in *Arabidopsis thaliana*, where phytochelatins, reductases and transporters derived from other species were integrated for heavy-metal removal²⁴. With the advent of molecular biology, there have been studies of several hundred genetic systems that have leveraged GMOs to degrade waste for bioremediation applications^{21,25}. Although promising, research to now has had limited success with GMOs for bioremediation due to the complex reactions involved and the ill-defined environments that these organisms have to tolerate and remediate in²⁵.

To avoid the technical hurdles of engineering SRMs or expressing foreign pathways in either bacteria or plants, a more tractable biological platform was used in this study to develop a bioremediation system for heavy-metal removal. Using an organism that

could easily be used by both scientists and non-scientists, in addition to having an established presence in industrial and consumer settings, was prioritized. Therefore, yeast was chosen. The common baker's yeast, *Saccharomyces cerevisiae*, is widely used in both scientific and consumer settings, and by using yeast, advantages beyond the biotechnology, such as infrastructure to scale, cost, packaging and transport, are already in place^{26–28}. The goal of this work was to transform yeast into a bioremediation platform for heavy-metal removal and tap into the available resources for translating yeast into a usable system for practical waste remediation and recycling in real-world settings. Rather than assembling complex metabolic circuits or introducing foreign genes, yeast's natural metabolic pathways were engineered to endogenously generate H₂S to concentrations similar to those produced by SRMs. However, unlike SRMs, sulfide production was controlled both in rate and overall production by modifying the sulfate assimilation pathway. These engineering steps endowed these yeasts with metal sulfide precipitation capabilities. In addition, controlling sulfide production helped control for precipitate size distribution and crystallinity, which could potentially improve downstream filtration and recycling processes. Overall, these results show that yeast, an already environmentally friendly and sustainably grown organism conventionally used for food and beverages, could be used as an agent for heavy-metal detoxification.

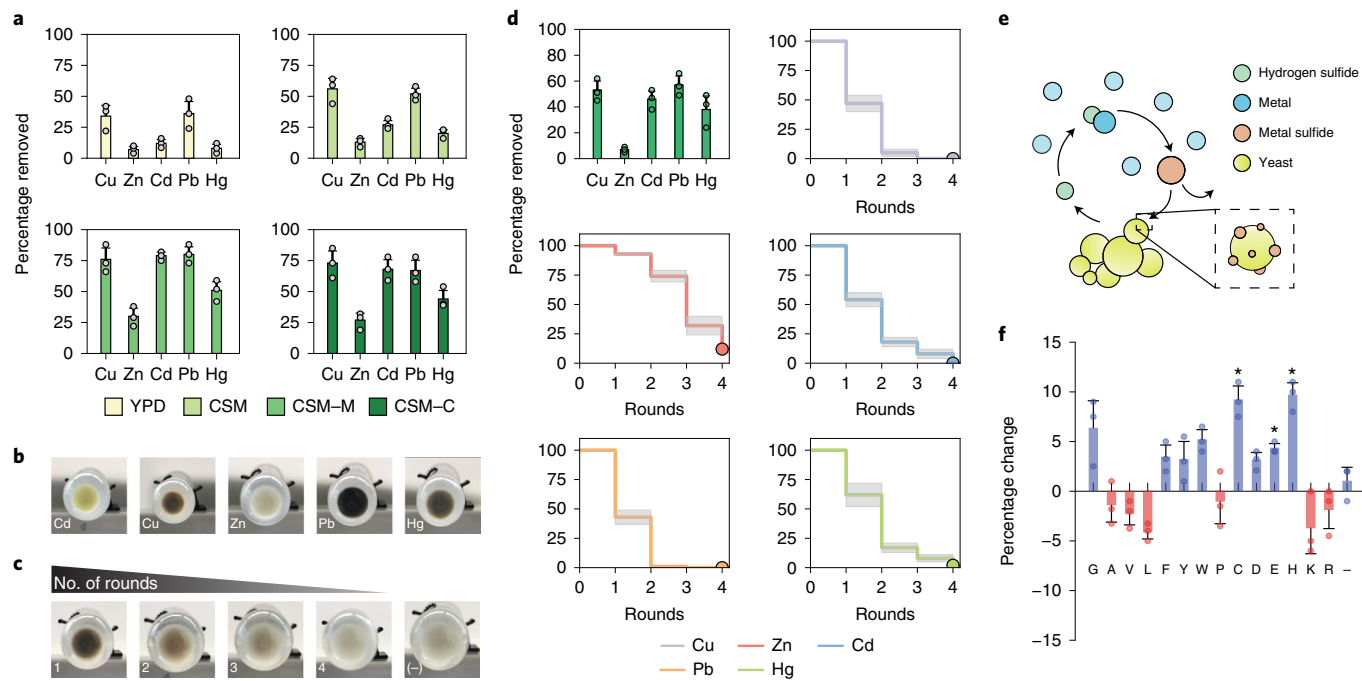


Fig. 2 | Uptake of Cu, Zn, Cd, Pb and Hg with $\Delta MET17$ sulfide-producing strains. **a**, Percentage precipitation of metals under varying culture conditions. -M and -C indicate media without methionine or cysteine, respectively. **b**, Visual representation of metal sulfide precipitation in cultures incubated with $100 \mu\text{M}$ metals. **c**, $\Delta MET17$ with Cu, Zn, Cd, Pb and Hg all at $100 \mu\text{M}$ were cultured together for multiple rounds of precipitation. Images represent sequential removal of metals via precipitation, with the darker precipitated colour gradually diminishing with increased number of rounds. (-) represents a yeast culture without any metals added. **d**, Data representing images in **c**. Top left plot represents the uptake from the first round. Remaining plots represent the gradual reduction of metal in solution after each round of precipitation. **e**, Illustration of the hypothesized reaction of metal sulfides on the yeast surface. Metals could precipitate either in solution or on the yeast surface. **f**, Percentage change in cadmium precipitation given expression of hexa-peptide repeats of the amino acids, and '-' as a control with no displayed peptides, designated on the x axis. For all data, the mean \pm s.d. of three replicates is shown.

Results

Engineering yeast to metabolically produce sulfide species. The metabolic transformation of sulfide to sulfate, sulfite and thiol functional groups requires complex multi-step reactions. Fortunately, the wine industry was key in elucidating much of the fundamental insights in controlling sulfide production, specifically H_2S . Good wine makers know that over-fermenting yeast can produce an off-putting egg smell, and scientists have identified the build-up of H_2S gas as the primary cause²⁹. Wine researchers recognized that the yeast sulfate assimilation pathway driven under fermentation conditions drove the production of H_2S gas (Fig. 1a)^{29,30}. Yeast wine strains were then engineered to suppress the production of H_2S for better-quality wine. However, by performing the opposite modifications, yeast's natural sulfide production was harnessed for heavy-metal sulfide-induced precipitation. During this investigation, it was shown that single gene knockouts in the sulfate assimilation pathway promoted H_2S production in a controllable manner. Knockout strains that produced detectable amounts of H_2S were $\Delta MET2$, $\Delta MET6$, $\Delta MET17$, $\Delta HOM2$, $\Delta HOM3$, $\Delta SER33$ and $\Delta CYS4$ (Fig. 1a). Specifically, $\Delta HOM2$, $\Delta MET17$ and $\Delta CYS4$ were chosen as experimental strains due to their consistently high levels of sulfide production and normal growth characteristics in complete synthetically defined media (CSM) compared with the other strains. From $\Delta HOM2$ and $\Delta MET17$ a double deletion was performed to obtain $\Delta HOM2$ and $\Delta MET17$ ($\Delta HM217$).

Despite the metabolic complexities of the sulfate assimilation pathway, yeast H_2S production was observed to follow Le Chatelier's principle. Supplying the necessary nutrients such as nitrogen sources and sulfate, while limiting the amount of 'products', that is, cysteine and methionine, stimulated the yeast sulfate assimilation

pathway to produce H_2S (Fig. 1b). The normal conversion of sulfide to thiol-containing biomolecules such as cysteine and methionine was retarded by removing pathway enzymes $\Delta CYS4$, $\Delta HOM2$ and $\Delta MET17$, thereby forcing expulsion of the intermediate H_2S . In CSM cultures, $\Delta CYS4$, $\Delta HOM2$, $\Delta MET17$ and $\Delta HM217$ produced $99 \pm 3 \text{ ppm}$ ($2.9 \pm 0.09 \text{ mM}$), $62 \pm 3 \text{ ppm}$ ($1.8 \pm 0.09 \text{ mM}$), $54 \pm 5 \text{ ppm}$ ($1.6 \pm 0.15 \text{ mM}$) and $133 \pm 3 \text{ ppm}$ ($3.9 \pm 0.09 \text{ mM}$) of sulfide species in a 50 ml flask culture, respectively (Fig. 1c and Supplementary Fig. 1a). Sulfide production was optimized by altering the media composition, primarily by removing cysteine and methionine. For $\Delta MET17$, sulfide production was tuned from a negligible amount to over $1,000 \text{ ppm}$ (approximately 30 mM) with a maximum production rate of $75 \pm 18 \text{ ppm}$ ($2.2 \pm 0.53 \text{ mM} \text{ h}^{-1}$) in 50 mL CSM cultures lacking methionine (Fig. 1d and Supplementary Fig. 1b,c).

Using sulfide-producing yeast for chemical precipitation. Cultures of $\Delta CYS4$, $\Delta HOM2$ and $\Delta MET17$ were incubated with $100 \mu\text{M}$ copper, zinc, cadmium, lead or mercury and shaken overnight. The amount of metal precipitated correlated to the strain's capacity to produce H_2S (Supplementary Fig. 1a), which could be tuned by altering culture conditions. Cultures grown in yeast extract peptone dextrose (YPD) precipitated the smallest amount of metals, whereas cultures grown in CSM lacking methionine or cysteine precipitated almost twice as much copper, cadmium, mercury and lead ($P < 0.05$) (Fig. 2a and Supplementary Fig. 2b). Culture density (OD) also affected the amount of metal precipitated. ODs at mid-log led to higher amounts of metal precipitation, primarily due to fast yeast growth rates, which corresponded to fast sulfide production rates (Fig. 1c and Supplementary Fig. 2c). Arsenate (AsO_4^{3-}) and chromate (CrO_4^{2-}) were also tested and were effectively precipitated

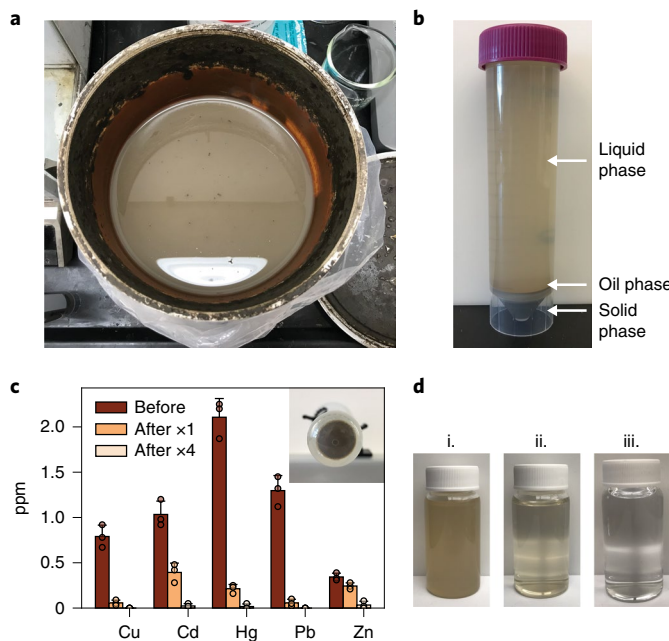


Fig. 3 | Treatment of effluent from the Athabasca oil sands using sulfide-producing yeast. **a**, Isolated effluent taken from the Athabasca oil sands. **b**, Effluent was centrifuged to separate the liquid, oil and solid phases, with the liquid phase used to test for yeast-induced metal precipitation. **c**, 1/1 mixture of liquid phase effluent to CSM-M culture with $\Delta MET17$ incubated overnight and measured for metal content. After one round, the supernatant was transferred to a fresh culture of $\Delta MET17$ and the experiment was repeated up to four times, with each iteration measured for metal content using ICP. The top right inlet image shows pelleted cell culture with precipitated waste after one round. **d**, Visual inspection of waste-water opacity before (i) and after (ii) one round of yeast-induced metal precipitation. iii, The same sample after four rounds of yeast-induced chemical precipitation. For all data, the mean \pm s.d. of three replicates is shown.

(Supplementary Fig. 3). However, the precipitation of arsenate and chromate were mainly due to their reduction into insoluble oxides rather than by direct sulfide precipitation.

When metals were mixed together, the preference for precipitation was copper, lead, cadmium, mercury and zinc in that order, loosely following their trends in solubility products and in line with observations from past physicochemical precipitation experiments^{5,20,31} (Fig. 2c,d). Rounds of precipitation, with unprecipitated metals transferred to fresh cultures, were tested to determine the minimum number of iterations required to completely remove metals from solution, a practice normally implemented in industrial water processing^{8,10,32,33}. Two rounds were required to remove copper and lead below 1% (1 μ M or 63 ppb and 207 ppb, respectively), three rounds for cadmium and mercury (below 1 μ M or 112 ppb and 201 ppb, respectively) and four rounds to remove zinc below 20% (20 μ M or 1.31 ppm) (Fig. 2c,d). These results closely approached US Environmental Protection Agency (EPA) standards for potable waters (that is, tens to hundreds of ppb)^{34,35}.

Sulfide-producing yeast were also tolerant to high levels of metal concentrations, some as high as 100 μ M cadmium and lead. $\Delta MET17$ showed robust growth curves compared with control in metal-containing media (Supplementary Fig. 4a). In addition, cells that underwent metal precipitation were regrown without much change in growth rate (Supplementary Fig. 4b).

Yeast display affects the amount of metal precipitated. Yeast display technology was used to modify the yeast surface to test whether

changes in cell surface chemistry would promote further precipitation. Thiol and metal-binding moieties such as histidine increased precipitation of cadmium, zinc and mercury by 5–10% but were negatively affected by more hydrophobic residues such as valine and leucine (Fig. 2e,f and Supplementary Fig. 5). Precipitation of copper and lead was not as affected. A hypothesis was that the fast copper/lead sulfide reaction rates favoured precipitation in solution rather than the diffusion-limited process of nucleating onto the cell surface.

Engineered yeast can remove metal waste found in oil sands. Effluent from the Athabasca oil sands in Canada was received and subjected to yeast-induced metal precipitation. The Athabasca oil sands are a well-known deposit of bitumen and crude oil, and for almost 100 years the area has been a key resource for oils and fossil fuels, which still drive the global economy³⁶. Therefore, the area has been heavily mined and contaminated with human-driven excavations, drilling and mining leading to erosion, pollution and ecological damage, which have made the Athabasca oil sands an area in need of major remediation³⁷. A sample of the effluent was obtained (Fig. 3a) and fractionated with gentle centrifugation to separate the liquid phase from the solid debris (Fig. 3b).

Inductively coupled plasma (ICP) analysis revealed that the liquid phase from the Athabasca oil sands contained appreciable amounts of copper, cadmium, mercury, lead and zinc, with the more-toxic cadmium, mercury and lead being more abundant per weight (1–2 ppm or mg l⁻¹) (Supplementary Fig. 6). One round of yeast-induced chemical precipitation showed greater than 85% removal of copper, mercury and lead and 30–50% removal of cadmium and zinc (Fig. 3c). These results are consistent with past metal uptake experiments at 100 μ M (10–20 times more concentrated) and support the idea that these engineered yeasts can be just as effective at precipitating metals in real-world environments. After three rounds of yeast-mediated metal precipitation, the copper, cadmium, mercury, lead and zinc levels closely approached zero ($P < 0.05$). Visual examination of the remediated effluent revealed that the opacity of effluent dramatically reduced after just one round (Fig. 3d and Supplementary Fig. 7).

Controlling metal sulfide particle size and morphology. The resultant precipitated mass was another consideration to judge the sustainability of this yeast-based system. Typically in chemical precipitation, precipitates form large amorphous masses that are difficult to separate and are thus routinely dumped into landfills or burned^{8,10,32}. Therefore, another consideration was to control the morphology and crystallinity of precipitates as a means to improve downstream separation, recovery and possibly recyclability of converted metals.

Precipitate experiments in CSM lacking both methionine and cysteine with fast H₂S production rates above 50 ppm h⁻¹ led to precipitates characterized by amorphous structures with average sizes exceeding 1 μ m and size distribution spanning two to three orders of magnitude ($P < 0.05$) (Fig. 4a). The precipitates were also shown to damage the cell wall, as transmission electron microscopy (TEM) analysis of cell sections showed fragmented cell walls surrounded by large metal sulfide aggregates (Fig. 4a). As H₂S production rates slowed by supplementing cultures with methionine and cysteine, the average precipitate size began to decrease while uniformly nucleating onto the cell wall as examined under TEM and energy dispersive X-ray (EDX) (Fig. 4b and Supplementary Fig. 8a). Cultures in fully supplemented CSM with H₂S production rates below 10 ppm h⁻¹ produced particles with controlled size distributions of 5–50 nm for cadmium sulfide ($P < 0.05$) (Fig. 4c). In addition, purified particles had a 1/1 metal-to-sulfide stoichiometry (Supplementary Fig. 8b). A hypothesis for this phenomenon could be that slower H₂S production rates allowed metals time to diffuse and nucleate on to the yeast

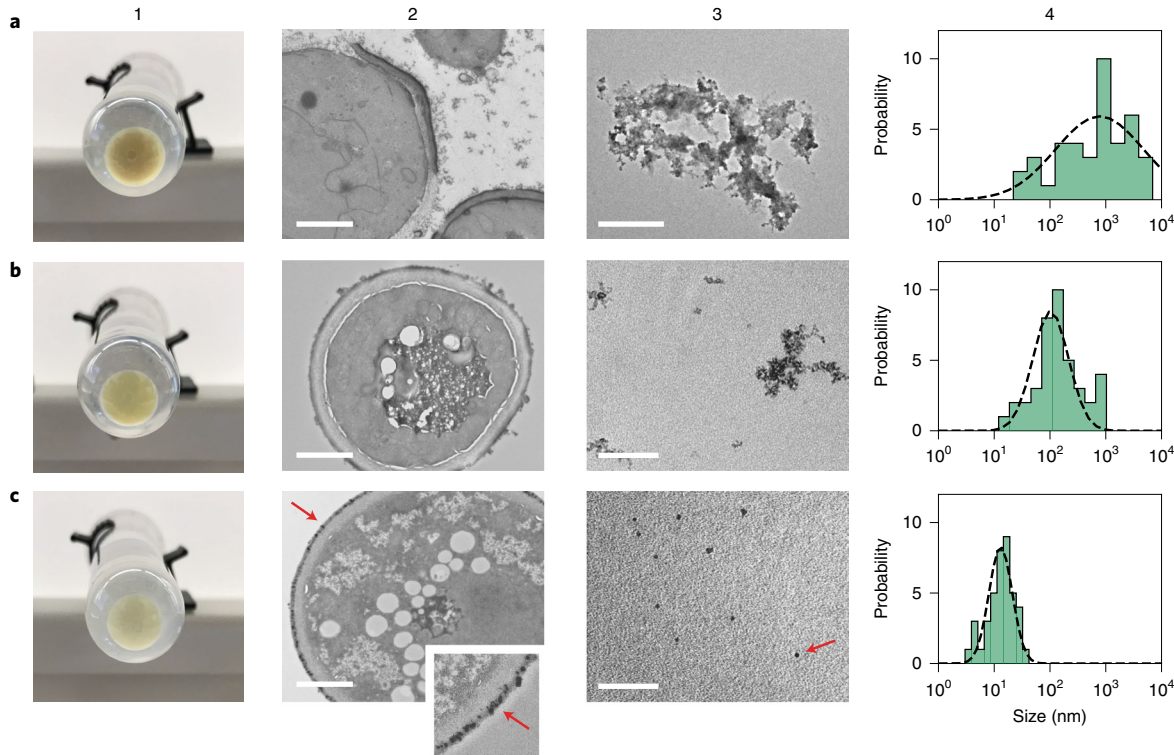


Fig. 4 | Controlled size distribution of cadmium sulfide particles by controlling sulfide production rates. Columns are ordered as follows: image of metal precipitate (1), cell sectioned with metal precipitates (2), isolated metal precipitate (3) and counted size distribution of isolated metal precipitate (4). **a**, Δ MET17 grown in CSM-M. **b**, Δ MET17 grown in CSM-C. **c**, Δ MET17 grown in CSM. The red arrows refer to the sub-50 nm precipitated nanoparticles, highlighting a single example of an isolated nanoparticle for each image subset. Column 2 scale bars are 1 μ m. Column 3 scale bars are 1 μ m (**a**) and 100 nm (**b,c**).

cell surface. Given that the cell wall consists of negatively charged polysaccharides and proteins, a reason could be that the electronegative environment allowed for somewhat size-controlled nucleation.

Recycling cadmium into cadmium sulfide nanoparticles. Metal nucleation was further explored by displaying nucleating peptides to facilitate metal sulfide growth, a concept that has been successfully employed in other biological organisms such as viruses and bacteria^{16,23,38,39}. Without any displayed motifs, precipitated cadmium sulfide examined under high-resolution TEM produced large amorphous structures (Fig. 5a). Crystalline structures indicated by lattice fringes were first observed with the hexa-cysteine motif, CCCCCC. More-prominent lattice fringes were observed with GGCAGC and GCCGCC displayed peptides, glycine–cysteine motifs generally conserved in metal-binding proteins such as metallothioneins⁴⁰ (Fig. 5a,b and higher-resolution images in Supplementary Figs. 9 and 10). Slowing the rate of sulfide production below 10 ppm h⁻¹ while displaying glycine–cysteine motifs generated cadmium sulfide quantum dot-like nanoparticles in the 10–50 nm range (Fig. 5c,d). With more crystalline features, these cadmium sulfide particles gave a strong excitation peak at 330 nm and an emission peak at 480 nm (Fig. 5e). In industry, cadmium sulfide nanoparticles are routinely used for their optical properties in light-emitting diodes (LEDs) and photovoltaics. Therefore, these results encourage the idea that there may be potential to convert precipitated metal sulfides into recyclable and useful materials. In addition, the ability to control for precipitate size and crystallinity, and developing a direct method for metal re-extraction through cell wall removal, could simplify downstream extraction and recycling⁴¹.

Considerations and feasibility in industrial settings. Yeast culture compositions are chemically defined and standard among scientists,

with yeasts being able to survive on several carbon sources at varying temperatures and at a pH as low as 3–4. In addition, yeasts grow in defined culture environments in both aerobic and anaerobic conditions. These factors have made yeast one of the most understood and appreciated organisms not only to scientists but also to bakers, beer makers and everyday consumers^{27,28}. A typical laboratory needs only US\$3.00 to produce one litre of yeast with respect to the cost of consumables such as glucose, extracts and buffers⁴². In industry, the infrastructure to scale and bioreactor optimization done by both the beer and pharmaceutical industries have reduced the cost to US\$0.16 per litre or less^{26,42,43}. These factors allowed a global production of more than one million tons of yeast by weight in 2015⁴⁴. More so, packaging and delivery of yeast through freeze-dried and active-dried packets have allowed the yeast market to touch all areas of the globe, allowing both high-tech industries and rural villages the power to brew their own yeast^{28,44}. If the scale and breadth of the yeast market can be tapped for bioremediation purposes, specifically the precipitation and conversion of heavy metals, then the potential impact on heavy-metal waste management can be profound.

Discussion

Future work will investigate more-complex displayed biomimetic peptides to improve metal sulfide formation and capture. Further design of biomimetic peptides could have two major applications: selective precipitation of metals and the creation of unique metal sulfide alloys that mimic doped metal sulfide compounds. Highly toxic elements such as cadmium and mercury in potable waters should be preferentially removed relative to less-toxic elements such as sodium or calcium. With engineered biomimetic peptides, it may be possible to selectively precipitate highly toxic metals such as mercury versus calcium even at

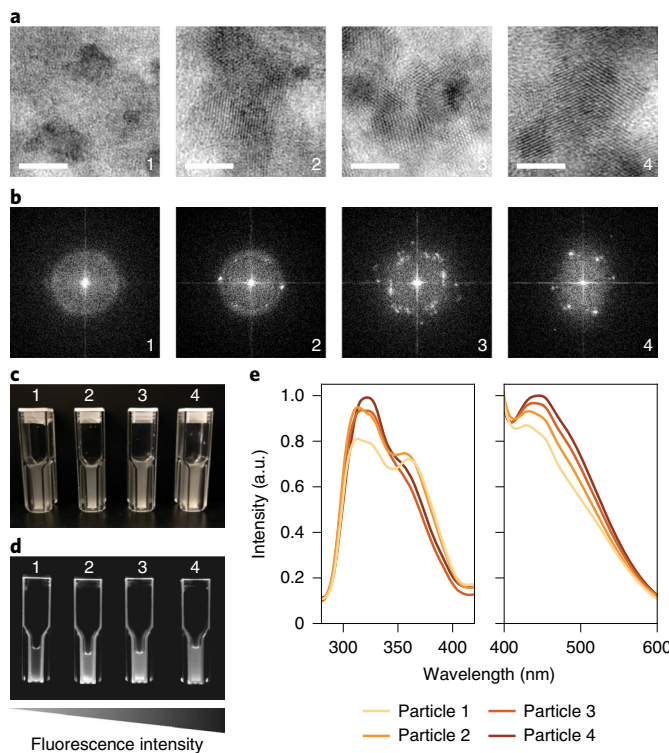


Fig. 5 | Analysis of isolated precipitated cadmium sulfide particles as a function of hexa-amino acid displayed peptides. Particle numberings: 1, GGGGGG; 2, CCCCCC; 3, GGCGGC; 4, GCCGCC. **a**, High-resolution TEM images of precipitated cadmium sulfide particles displaying various degrees of lattice fringes. Scale bars represent 5 nm. **b**, Fourier transform of cadmium sulfide particles showing various degrees of diffraction patterns caused by lattice fringes. **c**, Image of isolated cadmium sulfide suspended in water of samples 1 through 4 in ambient light. **d**, The same images captured under ultraviolet excitation. **e**, Excitation and emission spectra of samples 1 through 4. Excitation peak converged towards 330 nm and emission peak towards 450 nm with increasing crystallinity.

disproportionate concentrations by using known heavy-metal binding motifs found in nature^{16,38,39,45}. Another application is the ability to create useful metal sulfides in a ratiometric manner. Many metal sulfides used industrially are doped with other divalent metals to enhance their physicochemical properties in semiconductors, solar cells and magnetic materials^{46–48}. Therefore, engineering yeast to facilitate ratiometric precipitation of multi-metal sulfides is a concept that is especially interesting if the dopant metals are already present in the effluent.

More work is needed to design a pipeline for real-world bioremediation at scale. There are at least two primary strategies. The first is to grow yeast and securely package them into cartridges through size-exclusion filters or chemical cross-linking. These cartridges would maintain the optimal microenvironment for yeast to thrive and produce H₂S, for example salt, pH, nutrients and so on. The cartridges could then be fitted to a larger vessel that would enter a waste-contaminated area. As gaseous H₂S is produced, the surrounding environment would begin to precipitate heavy metals. Thorough investigation would be required to determine a cartridge's efficacy over time, such as the point at which a new cartridge should replace an old cartridge and how well the old cartridge's precipitated contents could be removed and recycled. An alternative solution would be to bring effluent to a treatment plant where waste is added to a yeast bioreactor. In this system, technologies from large-scale yeast fermentation could be leveraged to determine optimal fluid

control to move waste between multiple yeast beds for rounds of remediation^{26,42,43}. Similarly, these reactors would have separate controls to replenish reacted yeast and supply fresh cultures when needed. These processes are no different from traditional abiotic processes for mine effluent treatment. Current treatments use an assortment of chemical beds containing lime, iron and so forth that have high pH to precipitate heavy metals^{4,33}. Rather than relying on externally sourced chemicals for waste treatment, it would be more advantageous to use a renewable biological system such as yeast to control the reaction and by-products from treated waste waters.

Having yeast naturally produce sulfides is an attractive solution for curbing industry's reliance on mined sulfide gas. Currently, sulfide is produced from petroleum, natural gas and related fossil fuel activities, with China, the United States and Canada being leading producers^{49,50}. Sulfate, however, the metabolic precursor to H₂S in the yeast sulfate assimilation pathway^{29,30}, is generally more accessible through natural oxidation of ores, shales and agricultural runoff⁵¹, making sulfate more readily accessible than sulfide gas. Therefore, feeding yeast a low-value resource such as sulfate and generating a higher-value product such as H₂S could be a tremendous benefit for industry. These engineered yeasts provide a natural, environmentally responsible, low-cost H₂S source while also simplifying H₂S storage and transportation. Currently, H₂S storage is hazardous and costly, but with a yeast-based system, storing H₂S is equivalent to storing yeast.

In conclusion, this work used yeast to generate H₂S to precipitate heavy metals from contaminated waters. Furthermore, production of H₂S was tuned through gene knockouts and modulating media conditions, thereby controlling the quantity of metal precipitation and precipitate morphology. Crystallinity of metal sulfides was also controlled through displayed biomimetic peptides, making these particles easier to extract. This work ultimately showed that yeast could be a viable platform for heavy metal waste remediation and metal re-extraction and invites the exploration of other yeast-facilitated bioremediation processes.

Methods

Yeast strain and culture. Yeast strain W303α was obtained from the Amon Lab at MIT. Synthetically defined dropout medium was made by combining 1.7 g l⁻¹ yeast nitrogen base without amino acid and ammonium sulfate (Fischer), 5 g l⁻¹ ammonium sulfate (Sigma), 1.85 g l⁻¹ dropout mix without methionine and cysteine (US Biological), 20 g l⁻¹ glucose (Sigma) and 10 m l l⁻¹ × 100 adenine hemisulfate stock (1 g l⁻¹) (Sigma). CSM was made by adding cysteine and methionine amino acids at a final concentration of 50 mg l⁻¹ (Sigma). Both synthetically defined dropout media and CSM were adjusted to pH 7 with NaOH. Mixtures were stirred and filtered through a .22 μm filter top (EMD). YPD medium was made by adding 10 g l⁻¹ yeast extract, 20 g l⁻¹ peptone (Fisher) and 20 g l⁻¹ glucose (Sigma) and filtered sterilized. Plates were made by adding 20 g l⁻¹ Bacto Agar (Fisher) and autoclaving.

Cloning strategy and yeast transformations. The pRS303 and pRS305 vectors were used to clone the HIS and LEU markers for gene deletions in W303α via homologous recombination. Single gene deletions of *SER33*, *SER1*, *SER2*, *HOM2*, *HOM6*, *MET2*, *MET6*, *MET17*, *CYS3* and *CYS4* were made by amplifying the LEU marker using polymerase chain reaction (PCR) with 30 bp of the appropriate up- and downstream overlaps to their respective gene target (Supplementary Table 1). Double mutants were created by amplifying the HIS marker with 30 bp of the appropriate overlap to the target gene and transformed into the single deletant strains (Supplementary Table 2).

A constitutive yeast display vector constructed in the Belcher lab named pYAGA contains the *AGA1* and *AGA2* gene downstream of a GAP promoter and upstream of a CYC1 terminator. Single-stranded sequences coding for hexapeptide repeats were ordered from IDT and annealed with sticky ends matching the BamHII and PmeI cloning sites of pYAGA (Supplementary Table 3). Hexapeptide sequences were phosphorylated with T4 PNK before ligation using T4 ligase (NEB). Circularized plasmids were transformed into chemically competent NEB ω following the recommended NEB protocol and selected using ampicillin.

Yeast transformations were performed using Frozen-EZ Yeast Transformation Kit II (Zymo). For deletions, transformed cells were plated onto YPD for 1–2 d and replica plated onto dropout media (HIS, LEU or both) to select for positive transformants. Otherwise, plasmid transformations were grown directly onto plates with the appropriate dropout media. Plasmid or genomic DNA was isolated

by using silica bead beating and phenol/chloroform (Sigma) extraction. Sequences were confirmed by amplifying the isolated DNA using PCR and sequencing the DNA fragment using QuintaraBio sequencing services.

Screening and quantifying H₂S gas production. Cultures were initially screened in 5 ml CSM cultures in 14 ml BD culture tubes with taped lead acetate hydrogen sulfide indicator strips (VWR). Cultures were grown at 30 °C over 1–2 d, and H₂S was detected when strips became darkened. Quantitative sulfide detection was monitored using Draeger hydrogen sulfide detection columns (VWR). The 50 ml cultures in 250 ml Erlenmeyer flasks were corked with a single-hole rubber stopper in which hydrogen sulfide columns were fitted. Cultures grew for 1–2 d and were visually inspected at specific time points to measure sulfide production. Knockouts ΔSER33 and ΔCYS4 became auxotrophic to cysteine while ΔHOM3 and ΔMET2 became slow growers on synthetically defined media. Combination knockouts with ΔCYS4 produced extremely slow growers.

OD₆₀₀ culture density measurements. Discrete time-point optical density measurements were performed using 2 ml non-frosted cuvettes (VWR) and a tabletop DU800 Beckman Coulter spectrophotometer measuring at 600 nm. Continuous growth curve studies were performed on a shaking 96-well BioTek Synergy 2 plate reader held at 30 °C with 100 µl cultures. Cultures were first diluted from overnights to <0.1 OD₆₀₀ and aliquoted into a 96-well round bottom plate (Cellstar) with the appropriate metal and concentration.

Quantifying metal precipitation. Liquid stocks of copper (II) chloride, zinc chloride, cadmium nitrate, lead nitrate and mercury (II) chloride (Sigma) were made at 100 mM in water. Metal precipitation studies were performed by diluting overnight cultures to varying culture densities in 5 ml of fresh culture containing 100 µM of metal. Cultures were grown overnight and spun down at 900g for 3 min in a swinging bucket rotor, and supernatant was collected for metal measurement. Metal content was measured on an Agilent ICP-AES 5100 following standard operating procedures. Trace concentrations of metal below 10 µM were measured on an Agilent ICP-MS 7900. If samples were to be diluted, they were diluted in 3% HNO₃ (Sigma) to fit within the dynamic range of ICP detection.

For all experiments, a sample of just medium with spiked metal (for example, 100 µM) was measured to act as a reference for the initial metal content of copper, zinc, cadmium, lead and mercury in the medium. Metal removal measurements were calculated by taking the ICP measurements of the supernatant and subtracting from this reference to give the quantity of metal precipitated.

Multiple uptake experiments were performed by resuspending 1 OD₆₀₀ of fresh yeast grown the previous day with the equivalent volume of supernatant from the current metal precipitation experiment. For example, after the first round, the supernatant was collected and transferred to a freshly spun down culture inoculated the day before to a final OD of 1. The precipitation experiment was performed again, making this the second round of precipitation. This process was repeated at most up to four times, with each iteration sampled for ICP measurement.

Quantifying metal removal from oil sand samples. Samples of effluent were taken from the Athabasca oil sands in Canada. Liquid was gently centrifuged at 1,000g for 30 min to fractionate liquid, oil and solid phases. The liquid phase was used as the waste medium to test for yeast-induced metal precipitation. Although not thoroughly investigated in this study, the oil phase contained many organics, aromatics and oils contributed from mined runoff. The solid phase contained a heterogeneous mixture of large debris, rocks and precipitates that were easily spun down during centrifugation or through size-exclusion filtration.

To prepare the precipitation experiments, an overnight of ΔMET17 was grown in CSM-M and spun down. Then 1 OD₆₀₀ per ml of cells was added to a 1-to-1 mixture of ×2 CSM-M (prepared by doubling all ingredients), and the liquid phase was extracted from the effluent. The mixture was incubated overnight for 12 h, spun down and visualized for precipitation. The supernatant was taken for ICP measurement for copper, cadmium, mercury, lead and zinc following the procedures explained in the preceding.

The liquid phase metal profile was studied using ICP. Commercial ICP multi-element standards were used to multiplex measurements in parallel (VWR or Agilent). Multiple dilutions of the liquid phase in 3% HNO₃ were performed (such as 1 to 1, 1 to 10 and so on) to determine the level of matrix effect, as the liquid phase contained other contaminants not accounted for in the standards and skewed readings. A 1-to-5 dilution gave consistent results and was used to calculate the concentrations of Na, Mg, K, Ca, Sr, Ba, Mn, Fe, Cu, Zn, Si, Cd, Pb, Hg, Cr, As.

Quantifying yeast display expression using flow cytometry. Displayed peptides were first cloned with a carboxy (C) terminus V5 tag followed by a stop codon in a constitutive AGA1 and AGA2 vector, which was called pYAGA. Cultures were grown to saturating OD and 0.5 OD₆₀₀ were taken for flow cytometry. Cells were washed and pelleted at 900g with PBS + 1% BSA. Primary antibodies against V5 (Life Technologies) were diluted 1/500 in PBS + 1% BSA and incubated at room temperature for 1 h. Secondary antibodies with AlexaFluor 488 were diluted 1/2,000 in PBS + 1% BSA and incubated at room temperature for 1 h. Cells were then

washed and diluted to 1e6 cells per ml for flow cytometry. Flow cytometry was performed on a BD FACS Canto or LSR II following standard operating procedure provided by the Koch Flow Cytometry Core. Yeast cell gating strategy followed: FSC-A and SSC-A were used to gate on cells. FSC-W and FSC-H were used to gate vertically oriented single cells (vertical singlets). SSC-W and SSC-H were used to gate horizontally oriented single cells (horizontal singlets). After gating on these three plots, single cells were measured on the basis of fluorescence (Supplementary Fig. 11). Cell counts were plotted against binned fluorescent intensity (x axis) creating a population distribution histogram of fluorescence (y axis).

Extraction and purification of precipitated metal sulfides. Overnight cultures of metals added to yeast were pelleted at 900g for 3 min. Cultures were washed and resuspended in 1 ml sorbitol citrate. Then 100 T Zymolyase (Zymo) was diluted 1 to 100 and added to the suspension and incubated for >1 h at 30 °C while shaking. Digested cells were pelleted at 900g for 3 min, and supernatant was removed or kept for later analysis of dislodged metal sulfide particles. Cells were resuspended with 1/1 water and oleic acid (organic layer; Sigma). Mixtures were spun down at 900g for 3 min to pellet cellular debris while allowing insoluble metal sulfide particles to remain in the organic layer. The organic layer was removed, and fresh oleic acid was introduced to further extract metal sulfide particles. This process was performed 1–3 times until coloration was completely transferred into the organic layer. Most organic solvents were observed to work (phenol:chloroform, hexane, octanol and so on); however, oleic acid was more cost effective, easier to handle and safer to use. Samples could be used immediately for analysis or concentrated by spinning down particles at maximum speed for 15 min and resuspended in a lower volume in either oleic acid or water.

Excitation and emission measurements using fluorometry. An Agilent Cary Eclipse Fluorescence Spectrophotometer was used to measure the fluorescence of the isolated metal sulfide particles using disposable polymethyl methacrylate acrylic cuvettes (VWR). Excitation and emission scans were performed following standard operating procedures provided by the Center of Material Science Engineering, MIT.

TEM sample prep. To preserve the cell wall for imaging, cells were not digested with zymolayse. Cell fixation, dehydration, embedding and sectioning followed osmium thiocarbohydrazide osmium (OTO) staining provided by the WhiteHead Institute, MIT⁵². The yeast cells were grown to an appropriate optical density and fixed with 2% glutaraldehyde, 3% paraformaldehyde and 5% sucrose in 0.1 M sodium cacodylate buffer (EMS) for 1 h. Pelleted cells were washed and stained for 30 min in 1% OsO₄, 1% potassium ferrocyanide and 5 mM CaCl₂ in 0.1 M cacodylate buffer. Osmium staining was followed by washing and staining in 1% thiocarbohydrazide. Pellets were washed and stained again in the reduced osmium solution. The cells were then stained in 2% uranyl acetate (EMS) overnight, serially dehydrated with ethanol and embedded in EMBED-812 (EMS). Sections were cut on a Leica EM UC7 ultra microtome with a Diatome diamond knife at a thickness setting of 50 nm and stained with 2% uranyl acetate and lead citrate. The sections were examined using an FEI Tecnai Spirit at 80 kV and photographed with an AMT CCD camera.

TEM and EDX analysis. TEM samples of purified metal sulfide particles were prepared on 400-mesh nickel Formvar grids (EMS) by dropping 10 µl of sample onto the grids for 5 min and wicking dry. TEM images were acquired on an FEI Tecnai at 120 V. Samples were also monitored by EDX spectroscopy to qualitatively determine the relative amounts of sulfide and metal. When necessary, for example with copper, the signal background was corrected by subtracting the spectrum with a region without any metal sulfide particles to deconvolve overlapping peaks from the copper grid. High-resolution TEM images were acquired on a JEOL2010F at 200 V to observe crystal spacing. A JEOL2010F was used for more resolved EDX elemental mapping of metal sulfide particles that nucleated on the cell wall.

Purified metal sulfide particles were analysed for size distribution and morphology using TEM. Size distribution data were determined by imaging 40 random locations on 3 separate samples of isolated metal precipitates using TEM. Particles below 100 nm were imaged on the higher resolution JEOL2010F at greater than ×100,000 magnification. Sizes were quantitatively measured using ImageJ, and distributions were plotted as histograms.

Figure creation. Raw data were collected and stored as csv or Excel file formats. Data were imported and analysed with Python using modules such as numpy, pandas and scipy. Plots were graphed with matplotlib.

Statistical analysis. Statistical parameters, including the definitions and values of *n*, s.d. and/or standard error, are reported in the figures and corresponding figure legends. When reporting significance, a two-tailed unpaired *t* test was performed between observations, and *P* values were reported in the text. The significance threshold was set to *P* < 0.05 for all experiments, or as specified in the text.

Reporting Summary. Further information on research design is available in the Nature Research Reporting Summary linked to this article.

Data availability

The datasets generated and analysed during the current study are available from the corresponding author upon request. The source data underlying Figs. 1c, 1d, 2a, 3c, 4a–c, 5e and Extended Data 2a, 2c and 3b are provided as a Source Data File.

Received: 20 September 2018; Accepted: 14 January 2020;

Published online: 17 February 2020

References

- Rucevska, I. et al. *Waste Crime–Waste Risks: Gaps in Meeting the Global Waste Challenge* (UNEP and GRID-Arendal, 2015); <https://go.nature.com/38RZ1cY>
- Balde, C. P., Forti, V., Gray, V., Kuehr, R. & Stegmann, P. *The Global e-Waste Monitor 2017: Quantities, Flows and Resources* (United Nations University, International Telecommunication Union and International Solid Waste Association, 2017).
- Statistics: All Mining* (CDC, 2018); <https://www.cdc.gov/niosh/mining/statistics/allmining.html>
- DeGraff, J. V. in *Understanding and Responding to Hazardous Substances at Mine Sites in the Western United States* (ed. DeGraff, J. V.) 1–8 (Geological Society of America, 2007).
- Fu, F. & Wang, Q. Removal of heavy metal ions from wastewaters: a review. *J. Environ. Manage.* **92**, 407–418 (2011).
- Kang, D. H. P., Chen, M. & Ogunseitan, O. A. Potential environmental and human health impacts of rechargeable lithium batteries in electronic waste. *Environ. Sci. Technol.* **47**, 5495–5503 (2013).
- Song, X., Hu, S., Chen, D. & Zhu, B. Estimation of waste battery generation and analysis of the waste battery recycling system in China. *J. Ind. Ecol.* **21**, 57–69 (2017).
- Kurniawan, T. A., Chan, G. Y. S., Lo, W.-H. & Babel, S. Physico-chemical treatment techniques for wastewater laden with heavy metals. *Chem. Eng. J.* **118**, 83–98 (2006).
- Barakat, M. A. New trends in removing heavy metals from industrial wastewater. *Arab. J. Chem.* **4**, 361–377 (2011).
- Gupta, K. V., Ali, I., A. Saleh, T., Nayak, A. & Agarwal, S. Chemical treatment technologies for waste-water recycling—an overview. *RSC Adv.* **2**, 6380–6388 (2012).
- Gavrilescu, M., Demnerová, K., Aamand, J., Agathos, S. & Fava, F. Emerging pollutants in the environment: present and future challenges in biomonitoring, ecological risks and bioremediation. *New Biotechnol.* **32**, 147–156 (2015).
- Singh, A. & Prasad, S. M. Remediation of heavy metal contaminated ecosystem: an overview on technology advancement. *Int. J. Environ. Sci. Technol.* **12**, 353–366 (2015).
- Gadd, G. M. Microbial influence on metal mobility and application for bioremediation. *Geoderm* **122**, 109–119 (2004).
- Wiatrowski, H. A., Ward, P. M. & Barkay, T. Novel reduction of mercury (II) by mercury-sensitive dissimilatory metal reducing bacteria. *Environ. Sci. Technol.* **40**, 6690–6696 (2006).
- Silver, S. & Phung, L. T. Genes and enzymes involved in bacterial oxidation and reduction of inorganic arsenic. *Appl. Environ. Microbiol.* **71**, 599–608 (2005).
- Picard, A., Gartman, A., Clarke, D. R. & Girguis, P. R. Sulfate-reducing bacteria influence the nucleation and growth of mackinawite and greigite. *Geochim. Cosmochim. Acta* **220**, 367–384 (2018).
- Gartman, A. et al. Microbes facilitate mineral deposition in bioelectrochemical systems. *ACS Earth Space Chem.* **1**, 277–287 (2017).
- Jong, T. & Parry, D. L. Removal of sulfate and heavy metals by sulfate reducing bacteria in short-term bench scale upflow anaerobic packed bed reactor runs. *Water Res.* **37**, 3379–3389 (2003).
- Kieu, H. T. Q., Müller, E. & Horn, H. Heavy metal removal in anaerobic semi-continuous stirred tank reactors by a consortium of sulfate-reducing bacteria. *Water Res.* **45**, 3863–3870 (2011).
- Neculita, C.-M., Zagury, G. J. & Bussière, B. Passive treatment of acid mine drainage in bioreactors using sulfate-reducing bacteria. *J. Environ. Qual.* **36**, 1–16 (2007).
- Lovley, D. R. Cleaning up with genomics: applying molecular biology to bioremediation. *Nat. Rev. Microbiol.* **1**, 35–44 (2003).
- Shiratori, T., Inoue, C., Sugawara, K., Kusano, T. & Kitagawa, Y. Cloning and expression of *Thiobacillus ferrooxidans* mercury ion resistance genes in *Escherichia coli*. *J. Bacteriol.* **171**, 3458–3464 (1989).
- Wang, C. L., Maratukulam, P. D., Lum, A. M., Clark, D. S. & Keasling, J. D. Metabolic engineering of an aerobic sulfate reduction pathway and its application to precipitation of cadmium on the cell surface. *Appl. Environ. Microbiol.* **66**, 4497–4502 (2000).
- Krämer, U. & Chardonnet, A. The use of transgenic plants in the bioremediation of soils contaminated with trace elements. *Appl. Microbiol. Biotechnol.* **55**, 661–672 (2001).
- Sayler, G. S. & Ripp, S. Field applications of genetically engineered microorganisms for bioremediation processes. *Curr. Opin. Biotechnol.* **11**, 286–289 (2000).
- Vieira, É. D., da Graça Stupiello Andrietta, M. & Andrietta, S. R. Yeast biomass production: a new approach in glucose-limited feeding strategy. *Braz. J. Microbiol.* **44**, 551–558 (2013).
- Worldwide Beer Production, 2016* (Barth-Haas Group, 2018).
- Value of the Yeast Product Market Worldwide from 2016 to 2022 (in Billions U.S. Dollars)* (PR Newswire, 2017).
- Swiegers, J. H. & Pretorius, I. S. Modulation of volatile sulfur compounds by wine yeast. *Appl. Microbiol. Biotechnol.* **74**, 954–960 (2007).
- Linderholm, A. L., Findleton, C. L., Kumar, G., Hong, Y. & Bisson, L. F. Identification of genes affecting hydrogen sulfide formation in *Saccharomyces cerevisiae*. *Appl. Environ. Microbiol.* **74**, 1418–1427 (2008).
- Rickard, D. & Luther, G. W. Metal sulfide complexes and clusters. *Rev. Mineral. Geochem.* **61**, 421–504 (2006).
- Bolong, N., Ismail, A. F., Salim, M. R. & Matsura, T. A review of the effects of emerging contaminants in wastewater and options for their removal. *Desalination* **239**, 229–246 (2009).
- Johnson, D. B. & Hallberg, K. B. Acid mine drainage remediation options: a review. *Sci. Total Environ.* **338**, 3–14 (2005).
- Table of Regulated Drinking Water Contaminants* (EPA, 2019).
- Secondary Drinking Water Standards: Guidance for Nuisance Chemicals* (EPA, 2019).
- Sparks, B. D., Kotlyar, L. S., O'Carroll, J. B. & Chung, K. H. Athabasca oil sands: effect of organic coated solids on bitumen recovery and quality. *J. Pet. Sci. Eng.* **39**, 417–430 (2003).
- Kelly, E. N. et al. Oil sands development contributes elements toxic at low concentrations to the Athabasca River and its tributaries. *Proc. Natl Acad. Sci. USA* **107**, 16178–16183 (2010).
- Sakimoto, K. K., Wong, A. B. & Yang, P. Self-photosensitization of nonphotosynthetic bacteria for solar-to-chemical production. *Science* **351**, 74–77 (2016).
- Sweeney, R. Y. et al. Bacterial biosynthesis of cadmium sulfide nanocrystals. *Chem. Biol.* **11**, 1553–1559 (2004).
- DeSilva Tara, M., Gianluigi, Veglia, Fernando, Porcelli, Prantner Andrew, M. & Opella Stanley, J. Selectivity in heavy metal- binding to peptides and proteins. *Biopolymers* **64**, 189–197 (2002).
- Kim, J. et al. Effects of various pretreatments for enhanced anaerobic digestion with waste activated sludge. *J. Biosci. Bioeng.* **95**, 271–275 (2003).
- Harrison, R. G., Todd, P., Todd, P. W., Rudge, S. R. & Petrides, D. P. *Bioseparations Science and Engineering* (Oxford Univ. Press, 2015).
- Hoek, P. V., Dijken, J. P. V. & Pronk, J. T. Effect of specific growth rate on fermentative capacity of baker's yeast. *Appl. Environ. Microbiol.* **64**, 4226–4233 (1998).
- Yeasts, Yeast Extracts, Autolysates and Related Products: The Global Market* (BCC Research, 2017).
- Rugh, C. L. et al. Mercuric ion reduction and resistance in transgenic *Arabidopsis thaliana* plants expressing a modified bacterial merA gene. *Proc. Natl Acad. Sci. USA* **93**, 3182–3187 (1996).
- Arai, T. et al. Cu-doped ZnS hollow particle with high activity for hydrogen generation from alkaline sulfide solution under visible light. *Chem. Mater.* **20**, 1997–2000 (2008).
- Parveen, A., Agrawal, S. & Azam, A. Band gap tuning and fluorescence properties of lead sulfide Pb0.9A0.1S (A: Fe, Co, and Ni) nanoparticles by transition metal doping. *Opt. Mater.* **76**, 21–27 (2018).
- Bhattacharya, S. & Chakraborty, D. Electrical and magnetic properties of cold compacted iron-doped zinc sulfide nanoparticles synthesized by wet chemical method. *Chem. Phys. Lett.* **444**, 319–323 (2007).
- Selim, H., Gupta, A. K. & Al Shoaibi, A. Effect of reaction parameters on the quality of captured sulfur in Claus process. *Appl. Energy* **104**, 772–776 (2013).
- Minerals Information: Sulfur* (USGS, 2018).
- Little, B. J., Ray, R. I. & Pope, R. K. Relationship between corrosion and the biological sulfur cycle: a review. *CORROSION* **56**, 433–443 (2000).
- Seligman, A. M., Wasserkrug, H. L. & Hanker, J. S. A new staining method (OTO) for enhancing contrast of lipid-containing membranes and droplets in osmium tetroxide-fixed tissue with osmiophilic thiocarbohydrazide (TCH). *J. Cell Biol.* **30**, 424–432 (1966).

Acknowledgements

We thank the Koch Institute Facilities, Center for Material Science Facilities (CMSE), the Whitehead Keck Microscopy Facility, as well as Y. Zhang (CMSE) and N. Watson (Keck) for assisting in TEM sample prep and imaging. We acknowledge the Amon Lab for helpful discussions and advice in setting up basic yeast experiments, specifically C. Brennan and S. Morrill. We also thank N. Eze for insightful discussions and paper editing. This work was supported by the Amar G. Bose Research Grant (G.L.S. and A.M.B.) and the NSF Graduate Fellowship (G.L.S.). Partial support for this research was provided by a core center grant P30-ES002109.

from the National Institute of Environmental Health Sciences, National Institutes of Health.

Author contributions

G.L.S., E.E.R. and A.M.B. conceived the study and designed experiments; G.L.S. performed and E.E.R. helped with experiments; G.L.S. analysed the data and assembled figures; G.L.S., E.E.R. and A.M.B. wrote the manuscript.

Competing interests

The authors declare no competing interests.

Additional information

Extended data is available for this paper at <https://doi.org/10.1038/s41893-020-0478-9>.

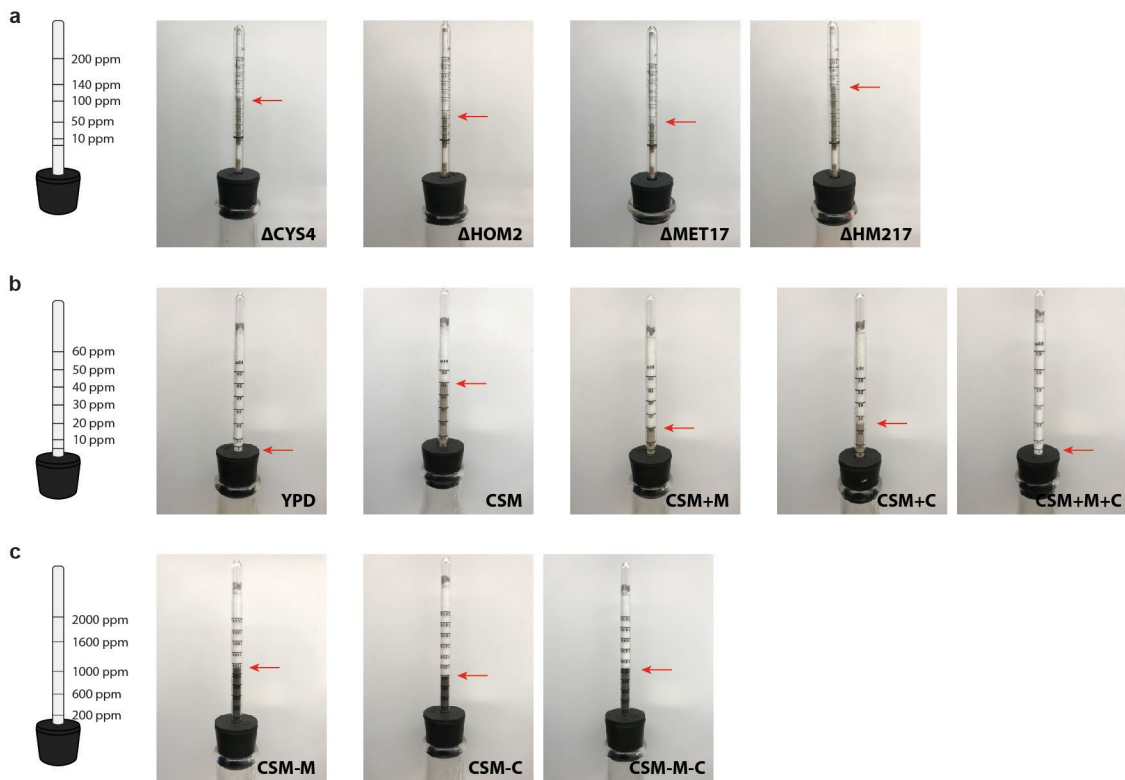
Supplementary information is available for this paper at <https://doi.org/10.1038/s41893-020-0478-9>.

Correspondence and requests for materials should be addressed to A.M.B.

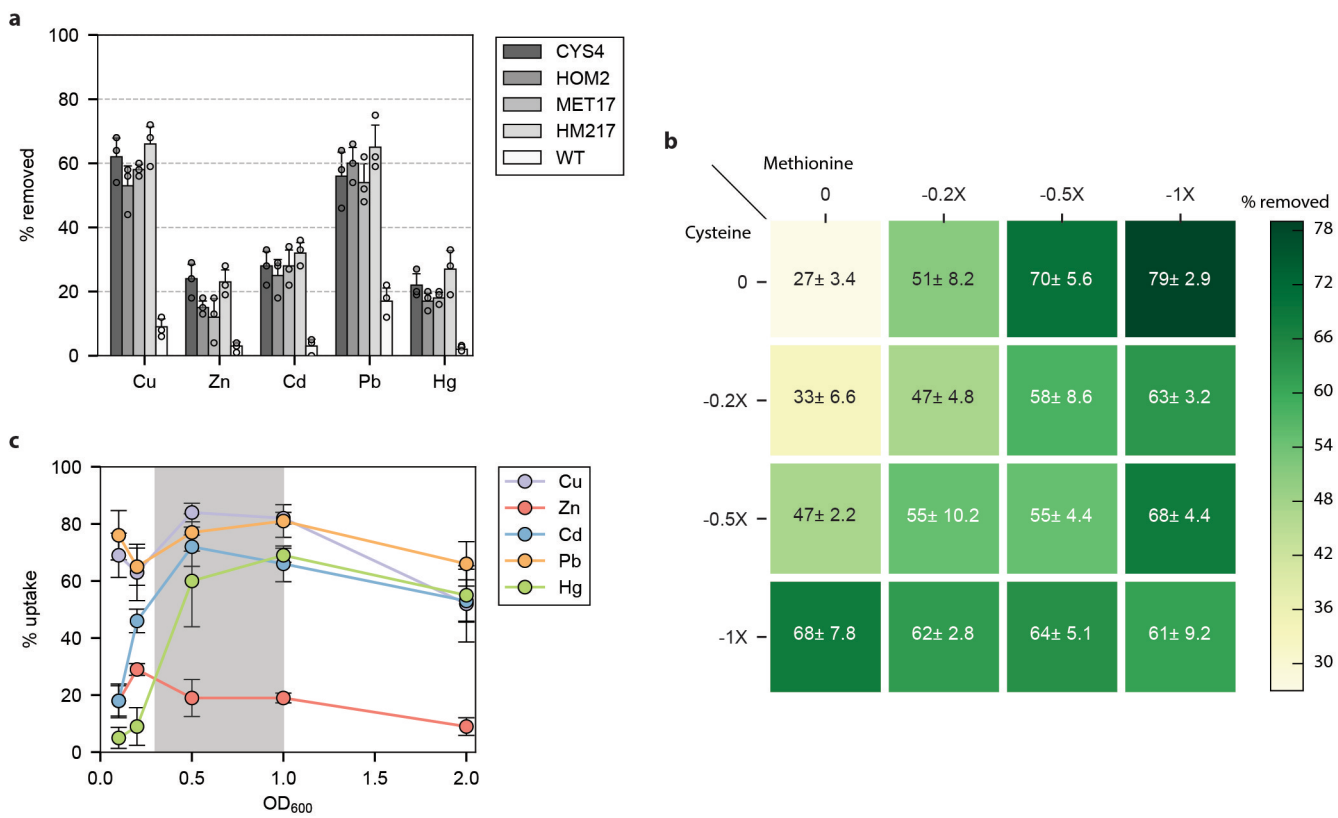
Reprints and permissions information is available at www.nature.com/reprints.

Publisher's note Springer Nature remains neutral with regard to jurisdictional claims in published maps and institutional affiliations.

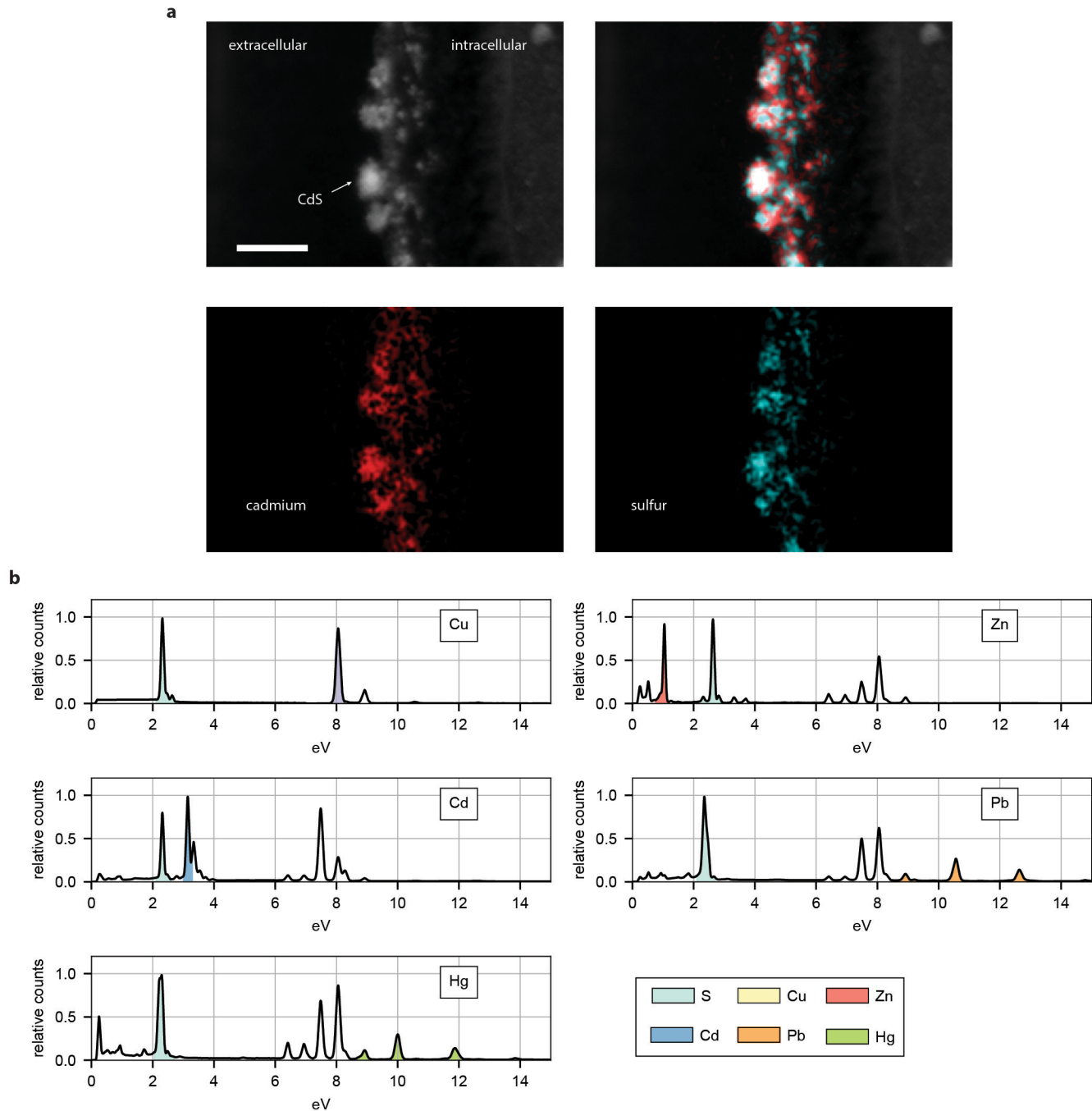
© The Author(s), under exclusive licence to Springer Nature Limited 2020



Extended Data Fig. 1 | Measuring yeast H₂S production. Illustrations left of the images represent H₂S detection columns with tick marks indicating the level of sulfide measured in ppm. **a**, Sulfide detection using 200 ppm columns for mutants Δ CYS4, Δ HOM2, Δ MET17, and Δ HM217. **b**, Sulfide detection using 60 ppm columns for Δ MET17 in cultures of YPD, CSM, and CSM with the addition (+) of methionine (M) or cysteine (C). **c**, Sulfide detection using 2000 ppm columns for Δ MET17 in CSM cultures lacking (-) methionine or cysteine, or both.



Extended Data Fig. 2 | Strain, culture density (OD₆₀₀), and media composition effects on metal precipitation. **a**, Precipitation of copper, zinc, cadmium, lead, and mercury with mutants Δ CYS4, Δ HOM2, Δ MET17, and Δ HM217, and WT as a control, in CSM. **b**, Effects of removing methionine (M) and/or cysteine (C) from CMS on precipitation efficacy using Δ MET17. Columns represent removal of M while rows represent removal of C from CSM. 1X stands for 100% removal (that is 0.2X = 20% and 0.5X=50%). Annotated values per cell grid represent the percent cadmium removed and standard error. **c**, Optimal culture density (marked within grey bounds) was determined by titrating cultures of Δ MET17 at different OD₆₀₀ with copper, zinc, cadmium, lead, and mercury. Metal color coding matches those used in the main text. For all data, the mean \pm s.d. of three replicates were taken for each data point.



Extended Data Fig. 3 | Elemental mapping of precipitated metal sulfide particles. **a**, Elemental mapping of HRTEM images of cadmium sulfide nanoparticles deposited on the cell wall of Δ MET17. Cadmium was false colored as red, sulfide as blue. Scale bars represent 50 nm. **b**, Elemental dispersive X-ray (EDX) spectroscopy was performed on purified precipitated copper, cadmium, lead, mercury, and zinc sulfide particles under TEM. Elemental K α peaks were colored and highlighted as areas under the curve for qualitative comparisons. Metal color coding of spectral plots match those used in the main text.

Corresponding author(s): Angela M. Belcher

Last updated by author(s): 12/20/2019

Reporting Summary

Nature Research wishes to improve the reproducibility of the work that we publish. This form provides structure for consistency and transparency in reporting. For further information on Nature Research policies, see [Authors & Referees](#) and the [Editorial Policy Checklist](#).

Statistics

For all statistical analyses, confirm that the following items are present in the figure legend, table legend, main text, or Methods section.

n/a Confirmed

- The exact sample size (n) for each experimental group/condition, given as a discrete number and unit of measurement
- A statement on whether measurements were taken from distinct samples or whether the same sample was measured repeatedly
- The statistical test(s) used AND whether they are one- or two-sided
Only common tests should be described solely by name; describe more complex techniques in the Methods section.
- A description of all covariates tested
- A description of any assumptions or corrections, such as tests of normality and adjustment for multiple comparisons
- A full description of the statistical parameters including central tendency (e.g. means) or other basic estimates (e.g. regression coefficient) AND variation (e.g. standard deviation) or associated estimates of uncertainty (e.g. confidence intervals)
- For null hypothesis testing, the test statistic (e.g. F , t , r) with confidence intervals, effect sizes, degrees of freedom and P value noted
Give P values as exact values whenever suitable.
- For Bayesian analysis, information on the choice of priors and Markov chain Monte Carlo settings
- For hierarchical and complex designs, identification of the appropriate level for tests and full reporting of outcomes
- Estimates of effect sizes (e.g. Cohen's d , Pearson's r), indicating how they were calculated

Our web collection on [statistics for biologists](#) contains articles on many of the points above.

Software and code

Policy information about [availability of computer code](#)

Data collection	Outputs from instruments or machines (e.g. ICP, plate readers) were exported or copied into a text readable format (e.g. .csv).
Data analysis	Excel and python were used to compile and analyze data. Open-source packages such as numpy, pandas, and matplotlib were used to quantify and graph results.

For manuscripts utilizing custom algorithms or software that are central to the research but not yet described in published literature, software must be made available to editors/reviewers. We strongly encourage code deposition in a community repository (e.g. GitHub). See the Nature Research [guidelines for submitting code & software](#) for further information.

Data

Policy information about [availability of data](#)

All manuscripts must include a [data availability statement](#). This statement should provide the following information, where applicable:

- Accession codes, unique identifiers, or web links for publicly available datasets
- A list of figures that have associated raw data
- A description of any restrictions on data availability

The datasets generated during and/or analyzed during the current study are available from the corresponding author on request.

Field-specific reporting

Please select the one below that is the best fit for your research. If you are not sure, read the appropriate sections before making your selection.

- Life sciences Behavioural & social sciences Ecological, evolutionary & environmental sciences

For a reference copy of the document with all sections, see nature.com/documents/nr-reporting-summary-flat.pdf

Life sciences study design

All studies must disclose on these points even when the disclosure is negative.

Sample size	Sample sizes of 3-5 were used in all experiments.
Data exclusions	No data or outliers were excluded in the results.
Replication	Metal uptake experiments were performed on samples prepared on separate days as well as measured on separate days when possible.
Randomization	Samples were not randomized during experimentation.
Blinding	Investigators were not blinded during the study.

Reporting for specific materials, systems and methods

We require information from authors about some types of materials, experimental systems and methods used in many studies. Here, indicate whether each material, system or method listed is relevant to your study. If you are not sure if a list item applies to your research, read the appropriate section before selecting a response.

Materials & experimental systems

- | | |
|-------------------------------------|--|
| n/a | Involved in the study |
| <input type="checkbox"/> | <input checked="" type="checkbox"/> Antibodies |
| <input checked="" type="checkbox"/> | <input type="checkbox"/> Eukaryotic cell lines |
| <input checked="" type="checkbox"/> | <input type="checkbox"/> Palaeontology |
| <input checked="" type="checkbox"/> | <input type="checkbox"/> Animals and other organisms |
| <input checked="" type="checkbox"/> | <input type="checkbox"/> Human research participants |
| <input checked="" type="checkbox"/> | <input type="checkbox"/> Clinical data |

Methods

- | | |
|-------------------------------------|--|
| n/a | Involved in the study |
| <input checked="" type="checkbox"/> | <input type="checkbox"/> ChIP-seq |
| <input type="checkbox"/> | <input checked="" type="checkbox"/> Flow cytometry |
| <input checked="" type="checkbox"/> | <input type="checkbox"/> MRI-based neuroimaging |

Antibodies

Antibodies used V5 Epitope Tag Antibody (2F11F7), Goat anti-Mouse IgG (H+L) Cross-Adsorbed Secondary Antibody Alexa Fluor 488.

Validation All antibodies were commercially purchased and validated.

V5 primary antibody: <https://www.thermofisher.com/order/genome-database/antibody/V5-Epitope-Tag-Antibody-clone-2F11F7-Monoclonal/37-7500>

Goat anti-Mouse secondary antibody Alexa Fluor 488: <https://www.thermofisher.com/antibody/product/Mouse-IgG-H-L-Secondary-Antibody-Polyclonal/A-11001>

Flow Cytometry

Plots

Confirm that:

- The axis labels state the marker and fluorochrome used (e.g. CD4-FITC).
- The axis scales are clearly visible. Include numbers along axes only for bottom left plot of group (a 'group' is an analysis of identical markers).
- All plots are contour plots with outliers or pseudocolor plots.
- A numerical value for number of cells or percentage (with statistics) is provided.

Methodology

Sample preparation	W303 yeast strains were grown on plates, transferred to liquid culture, and processed according to the methods section for experiments and analysis.
Instrument	BD FACS LSR II, BD FACS Celesta
Software	Python, with library FlowCytometryTools (https://eyurtsev.github.io/FlowCytometryTools/index.html)

Cell population abundance

Yeast strains were measured at 0.1 OD600, or roughly 1 million cells per mL.

Gating strategy

FSC-A and SSC-A was used to gate on cells. FSC-W and FSC-H was used to gate vertically orientated single cells (vertical singlets). SSC-W and SSC-H was used to gate horizontally orientated single cells (horizontal singlets). After gating on these 3 plots, single cells were measured for fluorescence.

Tick this box to confirm that a figure exemplifying the gating strategy is provided in the Supplementary Information.